The Astrophysical Journal, 937:62 (7pp), 2022 October 1 https://doi.org/10.3847/1538-4357/ac8df5

Lorentz Invariance Violation Test from Time Delays Measured with Gravitationally Lensed GRB Candidates 950830 and 200716C

Lin Lan[1], Aleksandra Piórkowska-Kurpas[2], Xudong Wen[1], Marek Biesiada[1,3], Kai Liao[4], He Gao[1], and Zhengxiang Li[1]
[1] Department of Astronomy, Beijing Normal University, Beijing 100875, People's Republic of China; gaohe@bnu.edu.cn
[2] Institute of Physics, University of Silesia, 75 Pułku Piechoty 1, 41-500 Chorzów, Poland
[3] National Centre for Nuclear Research, Pasteura 7, 02-093 Warsaw, Poland
[4] School of Physics and Technology, Wuhan University, Wuhan 430072, People's Republic of China
Received 2022 January 7; revised 2022 August 29; accepted 2022 August 29; published 2022 September 29

Abstract

The spectral lag features in gamma-ray bursts (GRBs) have been widely used to investigate possible Lorentz invariance violation (LIV). However, these constraints could depend on the unknown source-intrinsic time delays in different energy bands. Biesiada & Piórkowska theoretically proposed that gravitational lensing time delays in a strongly lensed GRB can become a tool for testing LIV free from the intrinsic time lag problem. Recently GRB 950830 and GRB 200716C have been proposed to be lensed by an intermediate-mass black hole. They should still be considered as candidates of strongly lensed bursts, since no angular offset (i.e., the evidence for multiple images) was detected, but only a double peak structure in the light curve. The redshift of the burst z_s and of the lens z_l have not been measured in either case; hence we assumed a reasonable guess of $z_l = 1.0$, $z_s = 2.0$ for GRB 950830 and $z_l = 0.174$, $z_s = 0.348$ for GRB 200716C. Bearing all this in mind, we attempted to constrain LIV theories in a prospective way based on the two GRBs by considering time delays between two pulses in different energy channels. By directly fitting the time delay data of GRBs 950830 and 200716C we obtained the following limits on LIV energy scale: $E_{\rm QG,1} \geqslant 3.2 \times 10^9$ GeV and $E_{\rm QG,1} \geqslant 6.3 \times 10^9$ GeV, respectively. Sensitivity analysis regarding the (unknown) redshifts leads to the most conservative estimate, $E_{\rm QG,1} \geqslant 1.5 \times 10^8$ GeV for GRB 950830 and $E_{\rm QG,1} \geqslant 4.8 \times 10^8$ GeV for GRB 200716C, when they would be located at $z_s \sim 5$.

Unified Astronomy Thesaurus concepts: Gamma-ray bursts (629)

1. Introduction

Lorentz invariance is the foundational symmetry of space-time in Einstein's relativity underlying two best known fundamental theories of nature: theory of gravity according to which the gravitational interaction is a consequence of curvature of spacetime and quantum field theory underlying the standard model of elementary particles. However, general relativity and quantum mechanics still remain to be unified within some, yet unknown, quantum gravity (QG) theories. A certain number of candidate QG scenarios have predicted that the Lorentz invariance violation (LIV) could manifest itself at a high-energy scale, expected to be of the order of the Planck energy scale $E_{\rm Pl} = \sqrt{\hbar c^5/G} \simeq 1.22 \times 10^{19}$ GeV (Kostelecký & Samuel 1989; Amelino-Camelia et al. 1997, 1998; Kostelecký & Mewes 2001; Mattingly 2005; Amelino-Camelia 2013; Tasson 2014). In such cases, photon velocity in a vacuum depends on its energy such that high-energy photons propagate slower (or faster) than low-energy ones (Amelino-Camelia et al. 1998). Hence, the energy scale for LIV (i.e., $E_{\rm QG}$) could be constrained from the differences in arrival times of the photons originating from the same astrophysical source measured in different energy bands (Amelino-Camelia et al. 1998; Ellis & Mavromatos 2013).

Gamma-ray bursts (GRBs) falling into two classes, short (duration <2 s) and long (duration >2 s) ones, are characterized by highly energetic photon emission detectable from large cosmological distances with some spectral lags in the prompt emission phase (Norris et al. 1986; Cheng et al. 1995; Norris et al. 1996; Band 1997; Peng et al. 2007; Shao et al. 2017; Lu et al. 2018) suggesting different arrival times of photons observed at different energy channels. The picture is that in most cases such lags are positive, which means that the peak of a GRB light curve registered at higher energies occurs earlier compared to those at lower ones with a smaller fraction of GRBs revealing null or even an inverse trend of the observed pulses (i.e., zero or negative spectral lags). A number of possible explanations can be found in the literature (see, e.g., discussion in Du et al. 2021 and references therein) but the true nature of such GRB features is not entirely clear. Being visible from very large cosmological distances, displaying short time variability in their light curves across some energy bands, GRBs have been widely used to constrain LIV theories (Amelino-Camelia et al. 1998; Ellis et al. 2006; Jacob & Piran 2008; Shao et al. 2010; Ellis & Mavromatos 2013; Kostelecký & Mewes 2013). For instance, various limits on LIV have been obtained using the observed time lags of single GRBs or a sample of GRBs (e.g., Schaefer 1999; Boggs et al. 2004; Ellis et al. 2006; Chang et al. 2012; Zhang & Ma 2015; Chang et al. 2016; Bernardini et al. 2017; Xiao et al. 2022). Particularly, some rare GRBs with high-energy photon emission (e.g., GRB 080916C, GRB 090510) or with the transition features from positive to negative lags in GRB lightcurve data at different energy bands presented more robust limits on LIV (e.g., Abdo et al. 2009a, 2009b; Xiao & Ma 2009; Nemiroff et al. 2012; Vasileiou et al. 2013; Pan et al. 2015; Wei et al. 2017a, 2017b; Acciari et al. 2020; Pan et al. 2020; Du et al. 2021).

However, the intrinsic effects caused by the unknown emission and acceleration mechanisms in the source could

mitigate or enhance the LIV-induced time delay, which would impact the accuracy of the resulting constraints on LIV. A key challenge is then to distinguish an intrinsic time lag at the source from a delay induced by LIV. Long GRBs usually have significantly positive or negative intrinsic spectral lags and should not be used for LIV searches until reasonable progress is made on the modeling of the emission and acceleration mechanisms (Chen et al. 2005; Ukwatta et al. 2012; Bernardini et al. 2015), while short GRBs are consistent with null or negligible intrinsic spectral lag and are therefore an ideal tool to measure the LIV effect (Norris & Bonnell 2006; Bernardini et al. 2015, 2017; Xiao et al. 2022). Currently, in addition to short GRBs, active galactic nucleus (AGN) flares and gamma-ray pulsars are two other classes of astrophysical sources that have no significant intrinsic lag in general and are often used for LIV tests (Biller et al. 1999; Kaaret 1999; Aharonian et al. 2008; MAGIC Collaboration et al. 2017). It should be noted, however, that there is also evidence of intrinsic lags in some cases of AGN flares and pulsars. For example, MAGIC Collaboration during an observational campaign regarding Mkn 501 blazar found an indication of about 4 minutes time delay between the peaks at $E < 0.25$ TeV and $E > 1.2$ TeV (MAGIC Collaboration et al. 2008), which may indicate a progressive acceleration of electrons in the emitting plasma blob. A robust method to study the correlations between arrival times and energy, based on a likelihood function built from the physical picture assumed for the emission, propagation, and detection of the photons was proposed by Martínez & Errando (2009). In the case of pulsars, there are some lags if the energy range is extended too much toward low energies (e.g., radio versus TeV). No real progress on the topic of intrinsic effects will be made without accurate models for production and acceleration mechanisms for each type of source. Perennes et al. (2020) first attempted to gain knowledge on source-intrinsic spectral lags of flaring AGNs at high and very high energies and on short timescales relevant for LIV searches, using leptonic AGN flare modeling. Concerning GRBs, some ways have been proposed to reduce the impact of intrinsic effects, e.g., fitting the observed spectral lags of statistical samples of GRBs at a range of different redshifts (Ellis et al. 2006; Bernardini et al. 2017; Xiao et al. 2022), or using only a limited observer-frame energy bands range corresponding to the fixed source-frame energy bands (Wei & Wu 2017). Anyway, there is no reason to think that the low and high-energy photons should be emitted simultaneously at the source, and while detecting distinct signals at different energy channels, we have no idea which one was sent first. Previous studies usually assumed that the intrinsic time delays are either an unknown constant for all GRBs considered or scale with the photon energy E according to some power-law function (Ellis et al. 2006; Biesiada & Piórkowska 2009a; Zhang & Ma 2015; Wei et al. 2017a; Acciari et al. 2020; Pan et al. 2020; Du et al. 2021).

In the context of testing LIV effects, an idea to mitigate the influence of the intrinsic effect has been formulated in Biesiada & Piórkowska (2009b), where it was argued that for gravitationally lensed GRB intrinsic time delays of lensed multiple signals (corresponding to multiple images of the source) it would be the same; hence the differences of lensing time delays in different energy bands could be attributed to LIV. This idea has been illustrated with galaxy lensing, where the lens was modeled as a singular isothermal sphere (SIS; Schneider et al. 1992). Since no case of GRB being lensed by a galaxy is known, this idea could not be tested against the data.

Recently, however, Paynter et al. (2021) claimed to identify a possible gravitationally lensed burst, GRB 950830 via Bayesian analysis of the BATSE lightcurve data set. They argued that the GRB was strongly lensed by an intermediate-mass black hole resulting in the observed light curve with two similar pulses separated by $\delta t \sim 0.39$ s. Furthermore, from temporal and spectral analysis, both Wang et al. (2021) and Yang et al. (2021) claimed that GRB 200716C is also a possible gravitationally lensed GRB. They considered that the GRB was strongly lensed by an intermediate-mass black hole based on the light curve with two similar pulses separated by $\delta t \sim 1.92$ s. Their inference was performed assuming the point-mass lens model from two GRBs. Most recently, Lin et al. (2022) presented a systematic search for millilensing of GRBs in the data from Fermi/Gamma-ray Burst Monitor (GBM), and more interesting candidates were proposed.

It is worth noticing that, in addition to a time delay, an angular offset (indication of multiple images) would be the smoking gun of gravitationally lensed GRBs. Unfortunately, for all these candidate lensed signals, no angular offset has been detected, suggesting that if there is an offset, it is smaller than the point-spread function of the instruments currently available. Moreover, there is no redshift measurement for the GRBs and no direct observation for the lens object. Therefore, it should be emphasized that these events are still candidates for strongly lensed GRBs. Interestingly, though, there have been noticeable differences in the gravitational lensing time delays between lensed images in different energy channels. Here we show, still in a prospective way, that if these differences could be attributed to LIV, they could be used to constrain LIV parameters independently of intrinsic time delays. We assume that the time delay and flux ratio of the GRBs 950830 and 200716C between two pulses in the lowest energy channel are due to the gravitational lensing time delay and magnification only (for the assumptions regarding redshifts, see Section 2).

This paper is organized as follows. The observed properties and time delay analysis for GRBs 950830 and 200716C are presented in Section 2. In Section 3, we present the methodology. Section 4 contains results and discussion. The conclusions are drawn in Section 5. Throughout the paper, a concordance cosmology (flat ΛCDM) with parameters $H_0 = 67.8$ km s^{-1} Mpc^{-1}, $\Omega_M = 0.308$, and $\Omega_\Lambda = 0.692$ has been adopted according to the *Planck* results (Planck Collaboration et al. 2018).

2. The Observed Properties and Time Delay Analysis for GRBs 950830 and 200716C

The short GRB 950830 was observed by BATSE on 1995 August 30 from the galactic coordinates $l = 344.^\circ6$ and $b = -45.^\circ4$. The prompt emission light curve consists of two alike pulses of duration $T_{90} = 0.544$ s separated by a quiescent gap. The event fluence (50–300 keV) in this time interval was $3.21^{+0.12}_{-0.12} \times 10^{-7}$ erg cm^{-2}, and the 1 s peak photon flux was $2.81^{+0.12}_{-0.12}$ ph cm^{-2} s^{-1} (Paciesas et al. 1999). The profiles of the two main pulses were so similar that the data preferred the fit with a single set of pulse parameters as compared to a more complex model with two completely independent pulses. Moreover, Paynter et al. (2021) analyzed the hardness of GRB 950830, which is defined as background photon counts in channel 3 (110–320 keV) to the counts in channel 2 (60–110 keV). They found that the hardness of the first pulse

(2.09 ± 0.10) and the second pulse (1.83 ± 0.11), were consistent within statistical errors. Similarly, Mukherjee & Nemiroff (2021) measured the flux ratio between these two pulses in four BATSE energy channels, and found that the flux ratios in different channels were also consistent within statistical errors.

The short GRB 200716C was observed by multiple satellites, including Swift/Burst Alert Telescope (BAT), Insight-HXMT, and Fermi/GBM. The GRB 200716C triggered the BAT at 22:57:41 UT on 2020 July 16 (Ukwatta et al. 2020); the prompt emission light curve consisted of two distinct pulses of duration ~5.3 s in the 15–150 keV band, and the event fluence (15–150 keV) in this time interval was $3.6^{+0.2}_{-0.2} \times 10^{-6}$ erg cm^{-2}, and the 1 s peak photon flux was $10.7^{+0.5}_{-0.5}$ ph cm^{-2} s^{-1}. The Fermi/GBM reported the detection of GRB 200716C at 22:57:41 UT on 2020 July 16 (Veres et al. 2020), the GBM light curve showed two prominent pulses with a total duration of ~5.3 s in the 50–300 keV band. The event fluence (10–1000 keV) in this time interval was $9.57^{+0.25}_{-0.25} \times 10^{-6}$ erg cm^{-2} and the 1 s peak photon flux was $19.3^{+0.3}_{-0.3}$ ph cm^{-2} s^{-1}. In addition, the Insight-HXMT/HE detected a GRB 200716C light curve consisting of two pulses with a duration ~2.16 s (Xue et al. 2020). Recently, Wang et al. (2021) and Yang et al. (2021) independently presented a Bayesian analysis of GRB 200716C in both temporal and spectral properties in different energy bands; they found that the hardness and flux ratio of the two main pulses in these bands were consistent within statistical errors.

These results could be interpreted as GRBs 950830 and 200716C being strongly lensed. Since gravitational lensing is achromatic and does not depend on photon energies, all lensed images of the source should have the same hardness and the gravitational lensing magnification (flux ratio) in each energy band (Paczynski 1986). Interestingly, the lensing time delays between two pulses in four energy channels display noticeable differences. If these differences were induced by the LIV effect, we would be able to test it free from the intrinsic time delay. It is unfortunate that these two GRBs did not have redshift measured. Paynter et al. (2021) argued that a mean BATSE GRB redshift of $\langle z_s \rangle \sim 2$ is a good guess based on the redshifts of known BATSE GRBs and the spectroscopically determined redshifts of other GRBs. Therefore they assumed the most probable configuration, with a lens at redshift $z_l \sim 1$ and a gamma-ray burst GRB 950830 at redshift $z_s \sim 2$. Wang et al. (2021) claimed that using the Amati relation $E_{\rm p} - E_{\gamma,\rm iso}$ one can assume that GRB 200716C could belong to the population of typical short GRBs at a redshift $z = 0.348$. Hence, a lens redshift $z_l \sim 0.174$ and a gamma-ray burst redshift $z_s \sim 0.348$ could be the most probable configuration for GRB 200716C.

Based on our assumptions, lensing time lag differences in different energy channels can be used to constrain LIV. To measure the time lags of temporally overlapping pulse signals of a gravitationally lensed system, the standard autocorrelation function (ACF) was used on binned GRB light curves. For GRBs 950830 and 200716C, we utilized the light curves from the time-tagged event data with 5 ms and 16 ms time bin resolution and obtained the corresponding ACF curves. In principle, if there are no similar pulses in the GRB light curves, the ACF curves should show a smoothly declining trend with the highest peak at time lag $\Delta t = 0$. Otherwise, if there are pairs of similar pulses with time lag Δt, the ACF curves are expected to show an effective peak around Δt. By adopting a third-order Savitzky–Golay smoothing filter to fit the ACF curves, the dispersion (σ) was defined between the ACF curves and the fitted Savitzky–Golay filter curves. As a rule, the highest effective peak exceeding 3σ was treated as evidence for the lensed GRB echo. The time lag Δt corresponding to the highest effective peak was measured and its uncertainty was estimated by adding Poisson noise to the original light curve. More details on data analysis with the ACF algorithm could be acquired from Paynter et al. (2021) and Wang et al. (2021). To sum up, we calculated the time lags of the two GRB light curves in different energy channels based on the ACF algorithm. For BATSE GRB 950830, we chose four fixed energy channels to measure the time lags by ACF analysis. We found the time delays between two pulses corresponding to channel 1 (20–60 keV), channel 2 (60–110 keV), channel 3 (110–320 keV), and channel 4 (320–2000 keV) to be 0.405 ± 0.001 s, 0.400 ± 0.002 s, 0.395 ± 0.002 s, and 0.385 ± 0.003 s, respectively. For Fermi GRB 200716C, we chose the five standard energy channels of Fermi/GBM to measure the time lags by ACF analysis. We obtained the time delays between two pulses corresponding to channel 1 (8–26 keV), channel 2 (26–85 keV), channel 3 (85–276 keV), channel 4 (276–900 keV), and channel 5 (900–40000 keV). They turned out to be 1.972 ± 0.002 s, 1.969 ± 0.003 s, 1.964 ± 0.008 s, 1.954 ± 0.018 s, and 1.947 ± 0.025 s, respectively. The observed time delays together with their energy bands are listed in Table 1. The two GRBs show positive time lags with high-energy photons preceding low-energy photons.

Table 1
The Gravitational Lensing Time Delays and Flux Ratios in Different Energy Bands for Millilensing Events

GRB Name	Energy Channels (keV)	$\Delta t_{\rm obs}$ (s)	r
950830	(20–60)	0.405 ± 0.001	1.079 ± 0.172
	(60–110)	0.400 ± 0.002	1.253 ± 0.071
	(110–320)	0.395 ± 0.002	1.543 ± 0.037
	(320–2000)	0.385 ± 0.003	0.995 ± 0.165
200716C	(8–26)	1.972 ± 0.002	1.334 ± 0.618
	(26–85)	1.969 ± 0.003	1.519 ± 0.455
	(85–276)	1.964 ± 0.008	1.595 ± 0.439
	(276–900)	1.954 ± 0.018	1.367 ± 1.014
	(900–40000)	1.947 ± 0.025	1.501 ± 0.433

3. Constraints on the LIV via Gravitational Lensing Time Delays

Gravitational lensing is the prediction of Einstein's general relativity following the fact that photons travel along null geodesics in spacetime whose curvature is induced by the distribution of mass and energy. Hence, the paths of photons emitted by a background source are distorted by massive objects in their way producing multiple images. One of the important consequences of gravitational lensing is the time delay between lensed images of the source. All these effects have been well confirmed for quasars and high redshift extragalactic radio sources lensed by galaxies. Because the GRBs are seen from large cosmological distances, one can expect that occasionally they could be gravitationally lensed. From the perspective of testing LIV theories the crucial issue is how lensing time delays depend on a photon's energy under a

LIV paradigm. So let us start with a reminder of the LIV time of flight delays.

3.1. LIV-induced Time Delays

Many approaches to quantum gravity predict the Lorentz invariance violation manifested as an energy-dependent modification of the relativistic dispersion relation for the photon:

$$E^2 - p^2c^2 = s_{\pm}E^2\left(\frac{E}{E_{\rm QG}}\right)^n, \quad (1)$$

where $E_{\rm QG}$ is the quantum gravity energy scale (still unknown, but often believed to be of the order of the Planck scale), n is the order of the specific LIV theory (we would assume later $n=1$), and $s_{\pm}$ is the sign parameter, with $s_{\pm}=+1$ corresponding to superluminal, and $s_{\pm}=-1$ to subluminal motion of high-energy photons (Amelino-Camelia et al. 1998). The dispersion Equation (1) leads to the Hamiltonian $\mathcal{H}=\sqrt{p^2c^2\left[1-\left(\frac{E}{E_{\rm QG}}\right)^n\right]}$, from which the photon's group velocity could be inferred as $v=\frac{\partial\mathcal{H}}{\partial p}$. In cosmological context this velocity will be time dependent (i.e., redshift dependent) since the photon's momentum p scales with the scale factor $a(t)$. To the first order in small parameter $E/E_{\rm QG}$ one has: $v(z)=c(1+z)\left[1-\frac{n+1}{2}\left(\frac{E}{E_{\rm QG}}\right)^n(1+z)^n\right]$. Therefore, one can attribute the comoving distance to the source at redshift z, which under LIV would be energy dependent:

$$r_{\rm LIV}(z)=\int_0^z\frac{c}{H(z')}\left[1-\frac{n+1}{2}\left(\frac{E}{E_{\rm QG}}\right)^n(1+z')^n\right]dz', \quad (2)$$

where $H(z)$ is the expansion rate (Hubble function) at redshift z. Physically this construction is a bit artificial, because the true comoving distance of the source is $r(z)$, but it is closely related to the time of flight difference $\Delta t=\Delta r_{\rm LIV}(z)/c$, where $\Delta r_{\rm LIV}(z)=|r_{\rm LIV}(z)-r(z)|$. This approach will be useful for calculations regarding strong lensing.

Introducing the notation

$$I_n(z_1,z_2)=\int_{z_1}^{z_2}\frac{(1+z')^n dz'}{h(z')}, \quad (3)$$

where $h(z)=H(z)/H_0=[\Omega_{\rm m}(1+z)^3+\Omega_\Lambda]^{1/2}$ is the dimensionless expansion rate, one may write $r_{\rm LIV}(z)=r(z)-\Delta r_{\rm LIV}(z)$, where $r(z)=\frac{c}{H_0}I_0(0,z)$ is the standard comoving distance of the source at redshift z, and the LIV correction is $\Delta r_{\rm LIV}(z)=\frac{c}{H_0}\frac{n+1}{2}\left(\frac{E}{E_{\rm QG}}\right)^n I_n(0,z)$. Furthermore, it would be useful to simplify expressions by introducing a small parameter ε:

$$r_{\rm LIV}(z)=r(z)[1-\varepsilon_{\rm LIV}(z)], \quad (4)$$

where:

$$\varepsilon_{\rm LIV}=\frac{n+1}{2}\left(\frac{E}{E_{\rm QG}}\right)^n\frac{I_n(0,z)}{I_0(0,z)}. \quad (5)$$

To summarize the issue of LIV-induced time delays: two photons with different energies (lower E_l and higher E_h; $E_h>E_l$) emitted from the same source at the same time would arrive to the observer at different times. From the preceding discussion, it follows that the LIV-induced time delay is given by Jacob & Piran (2008)[5]

$$\Delta t_{\rm LIV}=t_{\rm l}-t_{\rm h}=-\frac{n+1}{2}\left(\frac{E}{E_{\rm QG}}\right)^n\frac{I_n(0,z)}{H_0}, \quad (6)$$

where $t_{\rm l}$ and $t_{\rm h}$ are the arrival times of the low-energy photon and the high-energy photon, respectively.

3.2. Gravitational Lensing Time Delays

Let us consider a lens at redshift z_l. Gravitational lensing time delay functional at the (angular) position $\vec{\theta}$ on the lens plane can be calculated as

$$t(\vec{\theta})=\frac{1+z_l}{c}\frac{D_lD_s}{D_{ls}}\left[\frac{1}{2}(\vec{\theta}-\vec{\beta})^2-\psi(\vec{\theta})\right], \quad (7)$$

where $\vec{\beta}$ is (angular) position of the source (direction to the source in the absence of lensing), $\psi(\vec{\theta})$ is the projected gravitational potential, D_l and D_s are angular diameter distances to the lens and the source located at redshifts z_l and z_s, respectively, and D_{ls} is the angular diameter distance between the lens and the source. The angular diameter distances can be expressed by comoving distances $r(z_l)$ and $r(z_s)$ as

$$D_l=\frac{r(z_l)}{1+z_l};\ D_s=\frac{r(z_s)}{1+z_s};\ D_{ls}=\frac{r(z_s)-r(z_l)}{1+z_s}. \quad (8)$$

Because Paynter et al. (2021) fitted the GRB 950830 data to the point-mass lens, we will restrict ourselves to this particular model. This model is essentially different from the SIS model used in galaxy lensing studies. Hence, the results of this and the next section are complementary to those presented in Biesiada & Piórkowska (2009b).

The Einstein radius for the point-mass lens model reads

$$\theta_E=\sqrt{\frac{4GM_l}{c^2}\frac{D_{ls}}{D_sD_l}}, \quad (9)$$

where M_l is the mass of the gravitational lens. A point-mass lens produces a pair of images whose angular positions (with respect to the direction of the lens) are:

$$\theta_{\pm}=\frac{1}{2}(\beta\pm\sqrt{\beta^2+4\theta_E^2}) \quad (10)$$

and a lensing magnification of images reads

$$\mu_{\pm}=\frac{x_{\pm}^4}{x_{\pm}^4-1}=\frac{1}{2}\pm\frac{y^2+2}{2y\sqrt{y^2+4}}, \quad (11)$$

where $x_{\pm}=\theta_{\pm}/\theta_E$ and $y=\beta/\theta_E$. Introducing the flux ratio $r=|\frac{\mu_+}{\mu_-}|$, one can see that the following convenient expression

[5] Here, we only consider a simple LIV scenario with broken relativistic symmetries. Other more complex possibilities have been investigated, e.g., for the doubly special relativity (DSR) framework, in which relativistic symmetries are deformed rather than broken, and using a DSR lag–redshift relation would lead to smaller lags and lower limits (Rosati et al. 2015).

is valid (Mao 1992):

$$r = \left(\frac{\sqrt{y^2 + 4} + y}{\sqrt{y^2 + 4} - y} \right)^2. \tag{12}$$

This formula is particularly useful for expressing the unknown parameter y through measurable quantity r.

Finally, the lensing time delay between the two images produced by a point-mass lens can be given as

$$\Delta t_{\rm PM} = (1 + z_l) \frac{4GM_l}{c^3} f(y), \tag{13}$$

where

$$f(y) = \left(\frac{y}{2}\sqrt{y^2 + 4} + \ln \frac{\sqrt{y^2 + 4} + y}{\sqrt{y^2 + 4} - y} \right). \tag{14}$$

This, again, can be expressed by the flux ratio r:

$$\Delta t_{\rm PM} = \frac{2GM_l}{c^3}(1 + z_l)\left[\frac{r - 1}{\sqrt{r}} + \ln r \right]. \tag{15}$$

3.3. LIV-induced Time Delays and Gravitational Lensing Time Delays

Assume that we observe a GRB source at a cosmological distance emitting low-energy and high-energy photons, which undergoes gravitational lensing by a foreground intermediate-mass black hole. Then, we would observe a time delay (13) between the two images. According to standard physics this delay would be the same in each energy channel. If the LIV effects are present, we would again observe time delays. However, they would be a combined effect of lensing delays (13) and energy-dependent time of flight delays (6). In order to calculate a lensing time delay $\Delta t_{\rm LIV,PM}$ in the presence of LIV let us recall that, according to Equation (13), it depends on y expressed by the Einstein radius (9) related to comoving distances in the lensing system, which, in turn, are modified according to Equation (2). Using the expansion of $r_{\rm LIV}(z)$ to the first order in the $\varepsilon_{\rm LIV}(z)$ parameter one has

$$\theta_{E,\rm LIV} = \sqrt{\frac{4GM_l}{c^2}(1 + z_l)\frac{r_{\rm LIV}(z_s) - r_{\rm LIV}(z_l)}{r_{\rm LIV}(z_s) r_{\rm LIV}(z_l)}} \tag{16}$$

and the final result is

$$\theta_{E,\rm LIV} = \theta_E(1 + \varepsilon_{{\rm LIV},\theta}), \tag{17}$$

where

$$\varepsilon_{{\rm LIV},\theta} = \frac{n + 1}{4}\left(\frac{E}{E_{\rm QG}} \right)^n \times \left[\frac{I_n(0, z_l)}{I_0(0, z_l)} + \frac{I_n(0, z_s)}{I_0(0, z_s)} - \frac{I_n(z_l, z_s)}{I_0(z_l, z_s)} \right]. \tag{18}$$

Therefore, in the presence of LIV the Einstein radius would be energy dependent. For a point-mass lens, the difference between Einstein radii for high-energy and low-energy photons is $\Delta\theta_{E,\rm LIV} \coloneqq \theta_{E,\rm LIV} - \theta_E = \theta_E \frac{n+1}{4}\left(\frac{E}{E_{\rm QG}}\right)^n J_n(z_l, z_s)$, where we denote the term in brackets of Equation (18) as $J_n(z_l, z_s)$. In this case, the position of multiple images would be changed and the time delay between different images would also be altered and become energy dependent. Figure 1 shows how the function J_n varies with z_l and z_s for the linear (i.e., $n = 1$) and the quadratic (i.e., $n = 2$) LIV case.

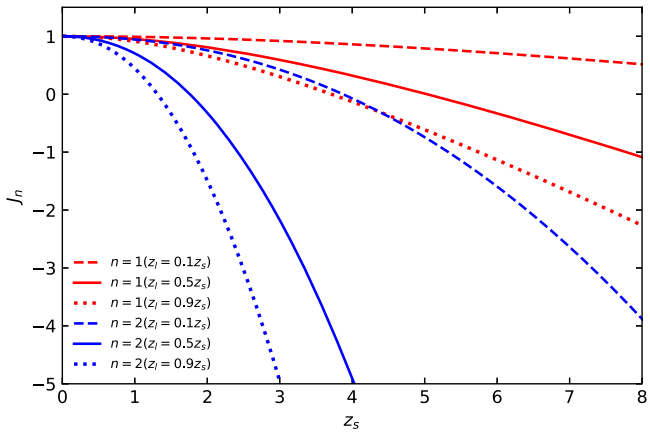

Figure 1. The quantity $J_n(z_l, z_s)$ as a function of source redshift z_s in different configurations of lens redshift z_l for the linear ($n = 1$) LIV model (red line style) and the quadratic ($n = 2$) LIV model (blue line style).

Equation (17) leads to the following form of y:

$$y_{\rm LIV} = y(1 - \varepsilon_{{\rm LIV},\theta}), \tag{19}$$

which plugged into Equations (13) and (14) gives the following correction:

$$\begin{aligned} f(y_{\rm LIV}) &= f(y) - y\sqrt{y^2 + 4}\,\varepsilon_{{\rm LIV},\theta} \\ &= f(y) - \frac{r - 1}{\sqrt{r}}\varepsilon_{{\rm LIV},\theta}. \end{aligned} \tag{20}$$

Fortunately, the LIV correction depends on the measurable flux ratio r. Finally the difference between LIV corrected and standard (i.e., low-energy) lensing time delays is:

$$\begin{aligned} \Delta_{\rm LIV}(\Delta t_{\rm PM}) &\coloneqq \Delta t_{\rm LIV,PM} - \Delta t_{\rm PM} \\ &= -\frac{4GM_l}{c^3}(1 + z_l)\frac{r - 1}{\sqrt{r}}\frac{n + 1}{4}\left(\frac{E}{E_{\rm QG}} \right)^n J_n(z_l, z_s). \end{aligned} \tag{21}$$

As already mentioned, we will assume the LIV order $n = 1$ while confronting above predictions with the GRB 950830 and 200716C data.

4. Results and Discussion

As a reminder, we assumed that the time delay and flux ratio of the GRBs 950830 and 200716C between two pulses in the lowest energy channel are due to the gravitational lensing time delay and magnification only. Using the observed time delay and flux ratio between two pulses in the lowest energy as the gravitational lensing time delay $\Delta t_{\rm PM}$ and magnification r, we could get the $(1 + z_l)M_l$ values by virtue of Equation (15). From the measured differences of gravitational lensing time delays in different energy channels and assumed source redshift, we finally determined the free parameter ($E_{\rm QG}$) using Equation (21).

The best-fitting theoretical curves for the linear LIV case (red solid line) are shown in Figure 2. With the best-fit value of $\log E_{\rm QG,1}$, the confidence-level lower limit on LIV for GRBs 950830 and 200716C are $E_{\rm QG,1} \geqslant 3.2 \times 10^9$ GeV and $E_{\rm QG,1} \geqslant 6.3 \times 10^9$ GeV, respectively. Because the two GRBs lack the data of higher energy photons (above GeV), our results are weaker than the limit for GRB 160625B and 190114C (Wei

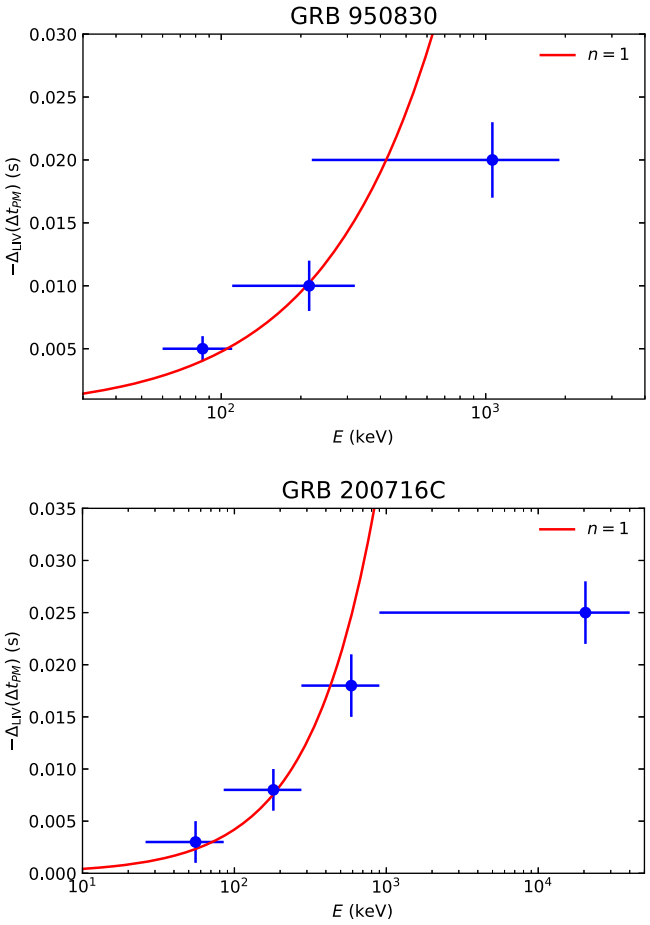

Figure 2. Energy dependence of the observed gravitational lensing time delays $\Delta_{\rm LIV}(\Delta t_{\rm PM})$ (relative to the softest energy band), and the best-fit theoretical curves (red solid line)—the linear ($n = 1$) LIV model.

et al. 2017a; Acciari et al. 2020; Pan et al. 2020; Du et al. 2021). But the advantage of our LIV results is in considering gravitational lensing time delays as a tool, which make this inference independent of intrinsic time lags. In our approach, we attribute all the differences in the gravitational lensing time delays between lensed images in different energy channels to LIV. In principle, however, part of the differences could also be induced due to the dispersion effect since different images experience different paths (dispersion effect should be very limited for γ-ray photons), or they could come from the illusion caused by the different response capabilities of satellites in different energy channels. These factors may increase the uncertainty of our results and weaken the limits on LIV. Here we only consider the point-mass lens model, which should be enough for the purpose of this work, since the inferred lens mass for both GRBs 950830 and 200716C although depending on the unknown lens redshift, falls into the mass range of intermediate-mass black holes (e.g., $\sim 10^4$–10^5 $M_\odot$). In the future, when galaxy-lensed GRBs are found and applied to constrain LIV, properties of the lens should be modeled more carefully (see Biesiada & Piórkowska 2009b for theoretical discussion on a LIV test by adopting other lens models). The lens modeling would, of course, introduce further uncertainties. Moreover, here we fix the cosmological model and its relevant parameters (see Section 1) to constrain LIV, which might cause additional uncertainties (Pan et al. 2015). The greatest uncertainty of our result comes from the unknown

Table 2
The Parameters and Results of the Sensitivity Analysis Regarding Redshifts of the Source and the Lens in the Linear LIV Scenario (i.e., $n = 1$)

GRB Name	z_s	z_l	M_l (10^5 $M_\odot$)	$J_n(z_l, z_s)$	$E_{\rm QG}$ (GeV)
950830	0.1	0.05	2.56 ± 0.63	1	4.8×10^9
	1	0.5	1.79 ± 0.44	0.953	4.0×10^9
	2	1	1.35 ± 0.33	0.810	3.2×10^9
	3	1.5	1.08 ± 0.27	0.592	2.6×10^9
	4	2	0.90 ± 0.22	0.321	1.8×10^9
	5	2.5	0.77 ± 0.19	0.01	1.5×10^8
	6	3	0.67 ± 0.17	−0.332	2.1×10^9
	7	3.5	0.60 ± 0.15	−0.699	3.3×10^9
	8	4	0.54 ± 0.13	−1.087	5.3×10^9
200716C	0.1	0.05	3.29 ± 0.83	1	6.8×10^9
	1	0.5	2.30 ± 0.58	0.953	6.1×10^9
	2	1	1.73 ± 0.44	0.810	5.7×10^9
	3	1.5	1.38 ± 0.35	0.592	5.2×10^9
	4	2	1.20 ± 0.29	0.321	4.2×10^9
	5	2.5	0.99 ± 0.25	0.010	4.8×10^8
	6	3	0.86 ± 0.22	−0.332	4.5×10^9
	7	3.5	0.77 ± 0.19	−0.699	5.8×10^9
	8	4	0.69 ± 0.17	−1.087	7.6×10^9

redshift of GRBs 950830 and 200716C. According to analysis in previous works, here we assume GRB 950830 at redshift $z_s \sim 2$ with a lens at redshift $z_l \sim 1$ and GRB 200716C at redshift $z_s \sim 0.348$ with a lens at redshift $z_l \sim 0.174$ (Paynter et al. 2021; Wang et al. 2021). In order to evaluate the uncertainty caused by the redshift assumption, we have performed a sensitivity analysis by assigning a wide range of redshifts for these two GRBs, from $z_s = 0.1$ to $z_s = 8$. For each case we used $z_l = z_s/2$ since it is a configuration close to the most probable one (i.e., the one that maximizes lensing probability). The parameters for the investigated scenarios are displayed in Table 2. Eventually, we found that when different redshifts are taken, limits on LIV from our method could vary within 1 order of magnitude, which could be taken as a systematic uncertainty for our results. According to the most conservative estimate, for a linear LIV case, we find $E_{\rm QG,1} \geqslant 1.5 \times 10^8$ GeV for GRB 950830 and $E_{\rm QG,1} \geqslant 4.8 \times 10^8$ GeV for GRB 200716C, when they are located at $z_s \sim 5$.

5. Conclusions and Prospects

GRBs have been viewed as one of the most promising sources for possible LIV studies due to their large cosmological distances and high-energy emission across wide energy bands. However the energy-dependent time of flight measurements, in principle, depend on the intrinsic time delays due to emission and acceleration mechanisms at the source. This could lead to systematic uncertainties on the LIV constraints in the flight-time method, which even though they are small, are still hard to assess. In this paper, we attempted to use two possibly gravitationally lensed GRBs 950830 and 200716C to eliminate the uncertainty of intrinsic time delays. By assuming that the differences of lensed GRB time delays between two pulses in different energy channels are induced by the LIV effect, we used the observed time delays of gravitational lensing for GRBs 950830 and 200716C to carry out precisely a test of LIV based on the point-mass model. For the linear LIV case, we found $E_{\rm QG,1} \geqslant 3.2 \times 10^9$ GeV and $E_{\rm QG,1} \geqslant 6.3 \times 10^9$ GeV for GRBs 950830 and 200716C, respectively.

It is worth noting that our limits are relatively weaker than the limits from previous works (Wei et al. 2017a; Acciari et al. 2020; Pan et al. 2020; Du et al. 2021). The advantage here, however, is that the intrinsic time delay does not influence our result. Previous studies usually assumed that the intrinsic time delays are either an unknown constant, the same for all GRBs considered, or that they scale with the photon energy E according to some power-law function (Ellis et al. 2006; Biesiada & Piórkowska 2009a; Zhang & Ma 2015; Wei et al. 2017a; Acciari et al. 2020; Pan et al. 2020; Du et al. 2021). In this case, the reliability of the resulting constraints are severely influenced by the assumption for intrinsic time delays. The current candidates of gravitationally lensed GRBs do not have high-energy (above GeV) detection. In the future, more observational data with higher temporal resolutions and reaching higher energies will be needed to get more stringent constraints on LIV.

The methodology we adopted requires data from lensed GRBs. Hence, it would be crucial to be able to detect such events. Besides their utility as probes of LIV theories, the transient nature of these events would allow precise time delay cosmography and studies of dark matter structure in lensing galaxies (Oguri 2019). The unique signature of strong gravitational lensing is the emergence of multiple images, which would appear as separate events with overlapping positional error boxes, identical time histories, and intensities that differ only by a magnification factor. This could be very demanding, since events associated with galaxy lenses would produce images with a separation of the order of a few arcseconds. Cluster lenses could produce images separated by $\sim 20''$, while lensing by the IMBHs would create images separated by $\sim 10^{-3}$ arcsec. This is much smaller than the resolution presently achievable. Therefore the search for a repeated signal in the light curve separated by several seconds, but not longer than a few minutes remains one of the most promising ways of identifying candidates of lensed GRBs. Another promising approach is to search for the optical counterpart of suspect lensed GRBs, e.g., its afterglow in X-ray, optical, and radio bands. If found it would confirm the lensed nature of the gamma-ray signal. While it is extremely difficult to achieve in the archival data, it could be promising if lensed GRB candidates were detected in ongoing or future surveys and triggered a concerted multifrequency follow-up.

We thank the anonymous referee for a very thorough analysis of the original version and extremely helpful comments that have helped us to improve significantly the presentation of the paper. This work is supported by the grant Nos. 12021003, 11973034, 11920101003 from the National Natural Science Foundation of China. M.B. was supported by the Key Foreign Expert Program for the Central Universities No. X2018002.

ORCID iDs

Marek Biesiada https://orcid.org/0000-0003-1308-7304
Kai Liao https://orcid.org/0000-0002-4359-5994
He Gao https://orcid.org/0000-0002-3100-6558
Zhengxiang Li https://orcid.org/0000-0002-8492-4408

References

Abdo, A. A., Ackermann, M., Ajello, M., et al. 2009b, Natur, 462, 331
Abdo, A. A., Ackermann, M., Arimoto, M., et al. 2009a, Sci, 323, 1688
Acciari, V. A., Ansoldi, S., Antonelli, L. A., et al. 2020, PhRvL, 125, 021301
Aharonian, F., Akhperjanian, A. G., Barres de Almeida, U., et al. 2008, PhRvL, 101, 170402
Amelino-Camelia, G. 2013, LRR, 16, 5
Amelino-Camelia, G., Ellis, J., Mavromatos, N. E., & Nanopoulos, D. V. 1997, IJMPA, 12, 607
Amelino-Camelia, G., Ellis, J., Mavromatos, N. E., Nanopoulos, D. V., & Sarkar, S. 1998, Natur, 393, 763
Band, D. L. 1997, ApJ, 486, 928
Bernardini, M. G., Ghirlanda, G., Campana, S., et al. 2015, MNRAS, 446, 1129
Bernardini, M. G., Ghirlanda, G., Campana, S., et al. 2017, A&A, 607, A121
Biesiada, M., & Piórkowska, A. 2009a, CQGra, 26, 125007
Biesiada, M., & Piórkowska, A. 2009b, MNRAS, 396, 946
Biller, S. D., Breslin, A. C., Buckley, J., et al. 1999, PhRvL, 83, 2108
Boggs, S. E., Wunderer, C. B., Hurley, K., & Coburn, W. 2004, ApJL, 611, L77
Chang, Z., Jiang, Y., & Lin, H.-N. 2012, APh, 36, 47
Chang, Z., Li, X., Lin, H.-N., et al. 2016, ChPhC, 40, 045102
Chen, L., Lou, Y.-Q., Wu, M., et al. 2005, ApJ, 619, 983
Cheng, L. X., Ma, Y. Q., Cheng, K. S., Lu, T., & Zhou, Y. Y. 1995, A&A, 300, 746
Du, S.-S., Lan, L., Wei, J.-J., et al. 2021, ApJ, 906, 8
Ellis, J., & Mavromatos, N. E. 2013, APh, 43, 50
Ellis, J., Mavromatos, N. E., Nanopoulos, D. V., Sakharov, A. S., & Sarkisyan, E. K. G. 2006, APh, 25, 402
Jacob, U., & Piran, T. 2008, JCAP, 2008, 031
Kaaret, P. 1999, A&A, 345, L32
Kostelecký, V. A., & Mewes, M. 2001, PhRvL, 87, 251304
Kostelecký, V. A., & Mewes, M. 2013, PhRvL, 110, 201601
Kostelecký, V. A., & Samuel, S. 1989, PhRvD, 39, 683
Lin, S.-J., Li, A., Gao, H., et al. 2022, ApJ, 931, 4
Lu, R.-J., Liang, Y.-F., Lin, D.-B., et al. 2018, ApJ, 865, 153
MAGIC Collaboration, Ahnen, M. L., Ansoldi, S., et al. 2017, ApJS, 232, 9
MAGIC Collaboration, Albert, J., Aliu, E., et al. 2008, PhLB, 668, 253
Mao, S. 1992, ApJL, 389, L41
Martínez, M., & Errando, M. 2009, APh, 31, 226
Mattingly, D. 2005, LRR, 8, 5
Mukherjee, O., & Nemiroff, R. J. 2021, RNAAS, 5, 103
Nemiroff, R. J., Connolly, R., Holmes, J., & Kostinski, A. B. 2012, PhRvL, 108, 231103
Norris, J. P., & Bonnell, J. T. 2006, ApJ, 643, 266
Norris, J. P., Nemiroff, R. J., Bonnell, J. T., et al. 1996, ApJ, 459, 393
Norris, J. P., Share, G. H., Messina, D. C., et al. 1986, ApJ, 301, 213
Oguri, M. 2019, RPPh, 82, 126901
Paciesas, W. S., Meegan, C. A., Pendleton, G. N., et al. 1999, ApJS, 122, 465
Paczynski, B. 1986, ApJL, 308, L43
Pan, Y., Gong, Y., Cao, S., Gao, H., & Zhu, Z.-H. 2015, ApJ, 808, 78
Pan, Y., Qi, J., Cao, S., et al. 2020, ApJ, 890, 169
Paynter, J., Webster, R., & Thrane, E. 2021, NatAs, 5, 560
Peng, Z.-Y., Lu, R.-J., Qin, Y.-P., & Zhang, B.-B. 2007, ChJAA, 7, 428
Perennes, C., Sol, H., & Bolmont, J. 2020, A&A, 633, A143
Planck Collaboration, Aghanim, N., Akrami, Y., et al. 2018, A&A, 617, A48
Rosati, G., Amelino-Camelia, G., Marcianò, A., & Matassa, M. 2015, PhRvD, 92, 124042
Schaefer, B. E. 1999, PhRvL, 82, 4964
Schneider, P., Ehlers, J., & Falco, E. E. 1992, Gravitational Lenses (Berlin: Springer)
Shao, L., Xiao, Z., & Ma, B.-Q. 2010, APh, 33, 312
Shao, L., Zhang, B.-B., Wang, F.-R., et al. 2017, ApJ, 844, 126
Tasson, J. D. 2014, RPPh, 77, 062901
Ukwatta, T. N., Barthelmy, S. D., Beardmore, A. P., et al. 2020, GCN, 28124, 1
Ukwatta, T. N., Dhuga, K. S., Stamatikos, M., et al. 2012, MNRAS, 419, 614
Vasileiou, V., Jacholkowska, A., Piron, F., et al. 2013, PhRvD, 87, 122001
Veres, P., Meegan, C. & Fermi GBM Team 2020, GCN, 28135, 1
Wang, Y., Jiang, L.-Y., Li, C.-K., et al. 2021, ApJL, 918, L34
Wei, J.-J., & Wu, X.-F. 2017, ApJ, 851, 127
Wei, J.-J., Wu, X.-F., Zhang, B.-B., et al. 2017a, ApJ, 842, 115
Wei, J.-J., Zhang, B.-B., Shao, L., Wu, X.-F., & Mészáros, P. 2017b, ApJL, 834, L13
Xiao, S., Xiong, S.-L., Wang, Y., et al. 2022, ApJL, 924, L29
Xiao, Z., & Ma, B.-Q. 2009, PhRvD, 80, 116005
Xue, W. C., Xiao, S., Yi, Q. B., et al. 2020, GCN, 28145, 1
Yang, X., Lü, H.-J., Yuan, H.-Y., et al. 2021, ApJL, 921, L29
Zhang, S., & Ma, B.-Q. 2015, APh, 61, 108